

CHAPTER 9

Interplay Between Physical and Chemical Events in Photoprocesses in Heterogeneous Systems

ALEXEI V. EMELINE*^{a,b}, VLADIMIR K. RYABCHUK^{a,b},
VYACHESLAV N. KUZNETSOV^b, AND NICK SERPONE*^c

^aLaboratory “Photoactive Nanocomposite Materials”, Saint-Petersburg State University, Ulyanovskaya Str. 1, Petergof, Saint-Petersburg, 198504 Russia;

^bFaculty of Physics, Saint-Petersburg State University, Ulyanovskaya Str. 1, Petergof, Saint-Petersburg, 198504 Russia; ^cPhotoGreen Laboratory, Dipartimento di Chimica, Università di Pavia, 27100 Pavia, Italy

*E-mail: emeline_av@hotmail.com

9.1 Introduction

Photophysical and photochemical processes in heterogeneous systems have been studied both intensively and extensively for many decades since the pioneering studies of Terenin and DeBeur in the early 1930s.^{1,2} The reason for such attention is quite simple: our world is a world of interfaces constantly exposed to the action of light. Consequently, numerous photostimulated processes in various natural and artificial heterogeneous systems play a very important role in our life starting from the origin of life and production of

RSC Energy and Environment Series No. 14

Photocatalysis: Fundamentals and Perspectives

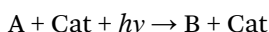
Edited by Jenny Schneider, Detlef Bahnemann, Jinhua Ye, Gianluca Li Puma, and Dionysios D. Dionysiou

© The Royal Society of Chemistry 2016

Published by the Royal Society of Chemistry, www.rsc.org

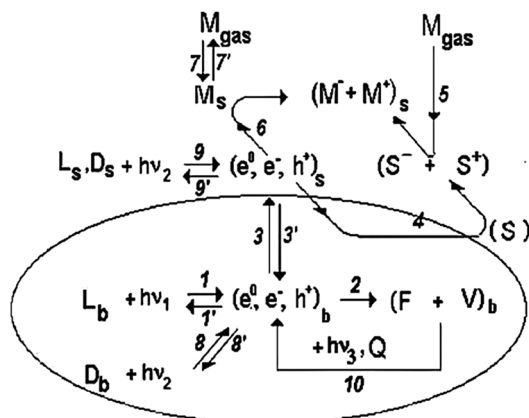
biomass as a result of natural photosynthesis to the problems of photosensitivity and/or photoresistance of modern materials, formation of self-cleaning surfaces, and environmental protection among others. As a fundamental and applied (technological) field of science, heterogeneous photochemistry and the related heterogeneous photocatalysis have attracted considerable attention from the chemical community in recent decades³⁻⁸ in the belief that they can resolve some of the problems connected, for example, with the chemical transformation and storage of solar energy, with environmental issues on the purification of water and air, with the artificial photosynthesis of important chemical products, and with the production of modern materials. Of particular interest is heterogeneous photocatalysis, principally because of the promising advantages that would result from the combination of photochemistry and heterogeneous catalysis.

In its simplest form, a heterogeneous photocatalytic (HPC) process can be defined briefly by the following reaction:



where A and B denote the chemical reagents and products, respectively, in the gaseous or liquid phase, and Cat refers to the solid photocatalyst that absorbs the incident light and on whose particle surface the photochemistry takes place. Two principal classes of heterogeneous photochemical processes can be delineated: stoichiometric photochemical reactions and photocatalyzed reactions. The above reaction embodies the generalization of a (i) non-catalytic chemical reaction ($A \rightarrow B$), (ii) heterogeneous catalysis {acceleration of the reaction rate with conservation of the catalyst {Cat: $A + \text{Cat} \rightarrow B + \text{Cat}$ }, and (iii) photochemistry that involves free energy for the process, $A + h\nu \rightarrow B$. When the catalytic cycle in process (ii) is incomplete (*i.e.* Cat is not restored or regenerated) the process then becomes a simple heterogeneous stoichiometric photochemical reaction (HSPR). Photostimulated adsorption (PA) can be taken as a certain type of HSPR. Concomitantly, PA is usually the initial step in both HPC and HSPR processes. Whatever the photochemical process, the initial steps of photoexcitation are similar, if not identical. In this context, we now consider the general mechanistic stages of interfacial photochemical processes/reactions that occur in gas/solid and liquid/solid heterogeneous systems as summarized in Scheme 9.1.

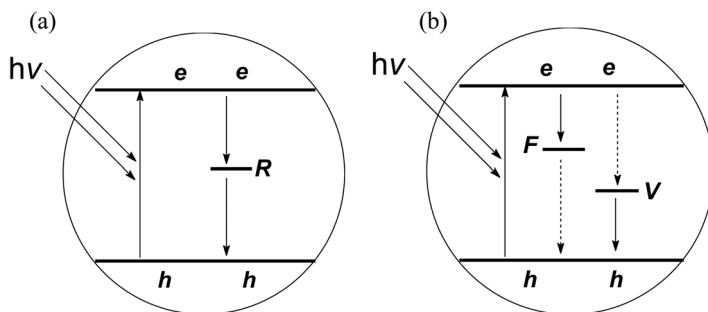
The driving force of such processes/reactions is absorption of the light free energy resulting in the intrinsic (band to band; stage 1) or extrinsic (ionization of defects; stage 8) excitation of the solid and the photoexcitation of surface states (stage 9), which lead to the photogeneration of charge carriers in the catalyst, namely electrons (e) and holes (h) in the conduction and valence bands, respectively. Since the positions of the energy levels of defects and surface states are within the forbidden energy gap (bandgap), photoexcitation (photoionization) of the defects and/or photoexcitation of the surface require photons with less energy compared to band-to-band photoexcitation ($h\nu_2 < h\nu_1$). Recombination (stages 1' and 9') and carrier trapping (stage 8')



Scheme 9.1 General mechanism of photoprocesses in heterogeneous systems.

events of excitation decay restore the initial state of the solid. Concomitantly, charge carriers can also be trapped partly by intrinsic and extrinsic defects in the solid (*e.g.*, anion and cation vacancies, V_a and V_c) to form new photoinduced defects (F-type and V-type color centers; stage 2) that alter the absorption spectrum of the solid by increasing the extrinsic absorption. In this regard, absorption of light by these photoinduced defects is redshifted compared to the original extrinsic absorption of the solid ($h\nu_3 < h\nu_2$). In addition, thermal excitation (Q) of photoinduced color centers can also generate free charge carriers (stage 10). Those carriers that reach the surface of the solid by diffusion and/or drift (stage 3; see below) can participate in interfacial charge transfer (redox) processes with pre-adsorbed species on the surface (stage 7) or with molecules in the gaseous phase. The chemical transformations at the surface begin after the photocarriers have been trapped by adsorbed molecules [the Langmuir–Hinshelwood (LH) model; stage 6] or by surface defect centers (S; stage 4) with subsequent collision with gaseous or solution phase molecules [the Eley–Rideal (ER) model; stage 5]. Accordingly, as evident from the general mechanism of Scheme 9.1, the charge carriers are the key players to initiate surface chemical transformations, and their behavior in the bulk and at the surface of the solid is the key that opens the pathway of photoreaction toward reduction or oxidation.

The appearance of photogenerated charge carriers indicates the transition of the photocatalyst to an excited state that is followed by relaxation processes causing the decay of the excitation energy. The photocatalyst retains its original state after photoexcitation *only* in the case of its complete relaxation to the original ground state. An example of such relaxation is presented in Scheme 9.2(a), which shows that photoexcitation of the solid photocatalyst results in the generation of free charge carriers in their conduction (electron) and valence (holes) bands, as a result of a band-to-band transition. Its relaxation occurs through *fast* recombination of charge carriers, either



Scheme 9.2 (a) Physical complete relaxation in photoexcited solids; (b) physical incomplete relaxation in photoexcited solids.

through band-to-band or through specific solid defects known as recombination centers (R).

As a result of such a complete recombination relaxation, the photocatalyst restores its original state after photo-irradiation is terminated. However, if for some reason relaxation through a recombination pathway is incomplete, then the photocatalyst does not return to its original state (Scheme 9.2b). In this latter case, the first step of relaxation involves the trapping of charge carriers by solid defects (*e.g.* anion and cation vacancies) in a manner otherwise identical to what happens in the first step of recombination through recombination centers (Scheme 9.2a) leading to formation of F- and V-type defects (the so-called color centers). However, the subsequent step of recombination of trapped charge carriers with the free charge carriers is much less effective (dashed arrows, Scheme 9.2b). This leads to an accumulation of trapped charge carriers and incomplete relaxation of the solid forming, as it were, a new metastable (excited) state of the photocatalyst that differs from the original one.

On the basis of the charge conservation law, clearly in the case of complete relaxation there remain no trapped charge carriers after termination of irradiation; that is, the concentration of trapped charge carriers is zero (eqn 9.1a and 9.1b):

$$[\mathbf{F}] = 0 \quad (9.1a)$$

$$[\mathbf{V}] = 0 \quad (9.1b)$$

where **F** and **V** denote the trapped electrons and holes, respectively. In the case of incomplete relaxation, the number of trapped electrons $[\mathbf{F}]$ equals the number of trapped holes $[\mathbf{V}]$; that is:

$$[\mathbf{F}] = [\mathbf{V}] \neq 0 \quad (9.2)$$

Because of the limited number of pre-existing defects in the solid, the kinetics of accumulation of trapped carriers becomes saturated. The level of saturation is determined by the efficiencies of charge carrier trapping and by

the decay of trapped carriers through different pathways that include recombination with free charge carriers of the opposite sign. Saturation of photocoloration of the metal-oxide specimen is achieved when:

$$\frac{d[\mathbf{F}]}{dt} = 0 \text{ and } \frac{d[\mathbf{V}]}{dt} = 0 \quad (9.3)$$

and $[\mathbf{F}]$ and $[\mathbf{V}]$ are given by eqn (9.4a) and (9.4b), respectively:

$$[\mathbf{F}] = \frac{k_{\text{tr}(e)}[e][V_a]}{(k_{\text{tr}(e)}[e] + k_{\text{tr}(h)}[h])} \quad (9.4a)$$

$$[\mathbf{V}] = \frac{k_{\text{tr}(h)}[h][V_c]}{(k_{\text{tr}(h)}[h] + k_{\text{tr}(e)}[e])} \quad (9.4b)$$

where $k_{\text{tr}(e)}$ and $k_{\text{tr}(h)}$ are the rate constants of trapping of electrons and holes by anion (V_a) and cation (V_c) vacancies, respectively, and $k_{\text{r}(h)}$ and $k_{\text{r}(e)}$ are the rate constants of recombination of free holes and electrons with \mathbf{F} - and \mathbf{V} -type color centers, respectively. Consequently, photocoloration of the solid specimen prevents the restoration of the original state of the photocatalyst, even when no surface reaction occurs.

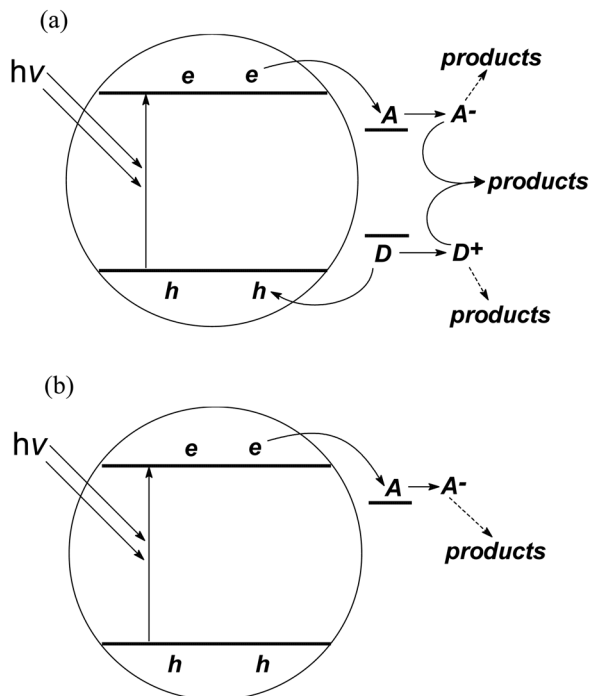
The ideal photocatalytic cycle is illustrated in Scheme 9.3(a). In this case, the photocatalyst returns to its original ground state in the same manner as in the case of internal charge carrier recombination in the solid. However, this time the relaxation processes take place through the external surface chemical reaction cycles. In general, it is not necessary for the reaction cycle to be a closed-loop process. It is sufficient that the number of electrons consumed by the electron acceptor A be equal to the number of electrons transferred to the catalyst by the electron donor molecules D, provided that the reaction products are not strongly bonded to the surface of the catalyst so as not to change the chemical composition of the metal-oxide surface. Obviously, the latter is also true for a photocatalytic process consisting of a closed-loop reaction cycle. In other words, the condition for true photocatalysis can be described by:

$$\frac{d[\mathbf{A}]}{dt} = \frac{d[\mathbf{D}]}{dt} \quad (9.5a)$$

or by:

$$\text{Rate}(\text{red}) = \text{Rate}(\text{ox}) \quad (9.5b)$$

That is, the rate of the surface reduction reaction that involves photogenerated electrons must equal the rate of the oxidation reaction that involves the photoholes. Otherwise, together with the occurrence of the catalytic process there would also be a non-catalytic surface chemical side-reaction determined by which half-reaction of the catalytic cycle is the more efficient.



Scheme 9.3 (a) Chemical complete relaxation of photoexcited solids; (b) chemical incomplete relaxation of photoexcited solids.

In addition, excess charge will accumulate in the solid. In the extreme case (Scheme 9.3b) when only one of the half-reactions takes place on the surface, the heterogeneous photochemical reaction is stoichiometric rather than photocatalytic. The simplest example of such a photochemical reaction is the photostimulated adsorption (*i.e.* photoreduction or photo-oxidation) of molecules on the surface of metal-oxide specimens.^{9,10}

Thus, the physical and chemical relaxation pathways compete with each other and a key role in such competition is played by the exchange of photo-generated charge carriers between these two pathways. Accordingly, this competition results in interplay between physical and chemical events in photoprocesses in heterogeneous systems. A few examples of such interplay are considered here.

9.2 Physical and Chemical Relaxation through Surface-Active Centers

In general, the reaction rate of a photocatalytic process can be expressed by eqn (9.6):¹¹

$$\left(\frac{dC}{dt}\right)_{\rho,C} = (\text{const})C^n\rho^m \quad (9.6)$$

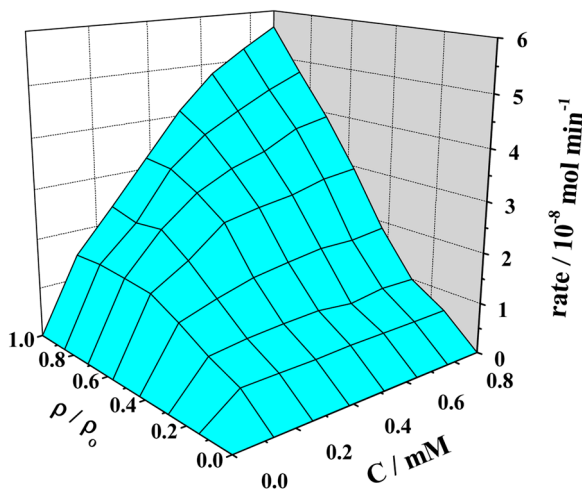


Figure 9.1 Three-dimensional dependence of the rate of phenol photodegradation over TiO_2 on its concentration (C) and on photon flow (ρ/ρ_0 ; $\rho_0 = 1.1 \times 10^{17}$ photons $\text{cm}^{-2} \text{s}^{-1}$ at $\lambda = 365$ nm) of the actinic light. (Reproduced from ref. 11. Copyright 2000 Elsevier.)

The results of kinetic studies [ER, LH] (Figure 9.1) of photostimulated processes in both liquid/solid and gas/solid heterogeneous systems show the interdependence of reaction rates on both light intensity and reagent concentration, which can be generalized by eqn (9.7):

$$\left\{ \frac{dC}{dt} \right\}_{\rho, C} = \frac{\alpha \rho C}{\beta \rho + \gamma C} \quad (9.7)$$

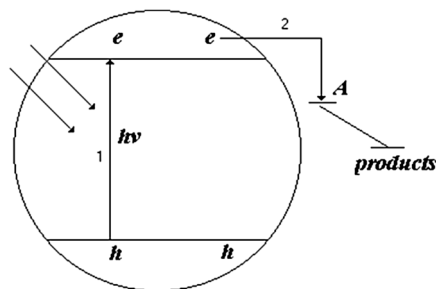
where the coefficients α , β , and γ are independent of light intensity and reagent concentration.

Hence, the necessary condition to determine the highest activity of a photocatalyst independent of reagent concentration at a given light intensity is $\gamma C \gg \beta \rho$. Under such conditions, to achieve the higher efficiency of the photocatalyst at lower concentrations of reagent requires a lower light intensity, thus indicating the existence of interplay between the physical process of photoexcitation and the chemical events in photoprocesses in heterogeneous systems.

To better understand those factors that determine the efficiency of heterogeneous photocatalytic processes, one should consider both bulk and surface processes in the photocatalyst, along with primary and secondary chemical surface reactions. The particular importance of the competition between physical and chemical relaxation processes through the surface defects – surface-active centers – is illustrated in Scheme 9.4.

For simple primary surface chemical reactions in the photo-oxidative process, we have:





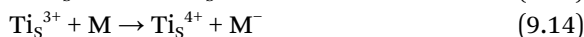
Scheme 9.4 Competition between physical and chemical relaxation processes through the surface defects – surface-active centers.



In the steady-state approach for the concentration of surface $\cdot\text{OH}_S$ radicals and charge carriers (electrons and holes), the reaction rate $d[\text{M}]/dt$ can be described as:

$$\left\{ \frac{d[\text{M}]}{dt} \right\}_{\rho, [\text{M}]} = \frac{k_{11}k_{13}[\text{h}_s^+][\text{OH}_S^-][\text{M}]}{k_{12}[e_s^-] + k_{13}[\text{M}]} \quad (9.11)$$

By analogy, a similar result can be obtained for the photoreduction reaction with participation of such electron surface-active centers as Ti_S^{3+} . Thus:



Eqn (9.10) and (9.14) represent the primary oxidative and reductive chemical events of the catalytic cycle. Eqn (9.8) and (9.12) show the generation of surface-active centers, whereas eqn (9.9) and (9.13) reflect the deactivation of such centers through the physical pathway. Both generation and deactivation of surface-active centers form the particular pathway of surface recombination of the free carriers.

Since the surface concentrations of free carriers are proportional to the intensity of the actinic light, eqn (9.11) is equivalent to the experimental dependence expressed by eqn (9.7) and demonstrates the interdependence of the reaction rate on a physical parameter (light intensity) and a chemical condition (concentration of reagent). The necessary condition $\gamma C \gg \beta \rho$ to observe the higher efficiency of the photocatalytic process is satisfied when $k_{13}[\text{M}] \gg k_{12}[e_s^-]$; that is, when the rate of chemical decay of the surface-active sites is much greater than the rate of their physical recombination process.

Note that at constant light intensity, which provides constant surface concentrations of free charge carriers, both eqn (9.7) and (9.11) can easily be transformed into the Langmuir–Hinshelwood (LH) kinetic equation, although strictly speaking the mechanism represented by eqn (9.8)–(9.10) corresponds to the Eley–Rideal (ER) mechanism. For the LH pathway, the notation M in eqn (9.10) represents the pre-adsorbed molecules of reagent whose concentration obeys the Langmuir adsorption isotherm:

$$[M_{\text{ads}}] = \frac{K[S_o][M]}{1 + K[M]} \quad (9.15)$$

The reaction rate expression is then given by:

$$\left\{ \frac{d[M]}{dt} \right\}_{\rho, [M]} = \frac{k_{11}k_{13}K[h_s^+][OH_s^-][S_o][M]}{k_{12}[e_s^-] + (k_{12}[e_s^-] + k_{13}[S_o])K[M]} \quad (9.16)$$

Eqn (9.16) can also be transformed into the classic LH equation at constant light intensity to demonstrate the interdependence of the reaction rate on light intensity and concentration of reagent. Thus, the competition between physical and chemical pathways of surface-active states deactivation determines the efficiency of the photochemical reactions at the photocatalyst surface.

At sufficiently high concentration of reagent, when the chemical reaction dominates the physical pathway of the surface recombination of carriers, the reaction rate is then equal to the rate of generation of surface-active centers (e.g., surface ·OH radicals for oxidative processes and electron centers (Ti³⁺) for reductive reactions) and it is proportional to the surface concentration of free charge carriers of the corresponding sign:

$$\frac{d[M]}{dt} = k_{11}[h_s^+][OH_s^-] \quad (9.17)$$

In other words, eqn (9.17) corresponds to the highest limit of photocatalyst activity. It cannot be overemphasized that this condition must be satisfied should one wish to compare the activities of different photoactive materials.

9.3 Photoinduced Defect Formation

One of the more interesting examples of the interplays between physical and chemical photoprocesses in heterogeneous systems is the effect of surface photochemical reactions on the photoinduced formation of defects in solids^{12–16} caused by the trapping of photogenerated charge carriers by *intrinsic* and *extrinsic* defects in solids,^{12–16} and by the self-trapping of excitons in regular lattice sites of photosensitive solids.^{13,14} The corresponding photophysical processes can be considered as photochemical redox reactions in solids that create new defects with higher reduced and/or oxidized states. Examples

of such processes are the photoinduced formation of $O^{\cdot-}$ and Ti^{3+} or Zr^{3+} states in titanium and zirconium oxides, respectively.^{10,15,16} Note that such processes take place regardless of the advent of surface photochemical reactions.^{10,16} Accordingly, a solid photocatalyst typically changes its state during the photo-irradiation event. Thermodynamically this corresponds to the creation of quasi-Fermi levels for the photoinduced defects that generally differ from the quasi-Fermi levels of the photogenerated free charge carriers (electrons and holes). Thus, with the photoinduced formation of new defects, the photocatalyst changes its thermodynamic state, and consequently does not possess the same state as the original state during or after irradiation. This is a typical situation in heterogeneous catalysis when the stationary state(s) of surface structure and composition of the catalyst during the catalytic process differ from the initial state.

The effect of surface photochemical reactions on the photoinduced formation of defects is based on the charge conservation law. In general, the fate of charge carriers in heterogeneous system can be summarized by eqn (9.18):

$$[e] + [e_R] + [e_{v_a}] + [e_v] + [e_A] = [h] + [h_R] + [h_{v_c}] + [h_F] + [h_D] \quad (9.18)$$

where (i) $[e]$ and $[h]$ are the numbers of photogenerated free electrons and holes, respectively – at moderate levels of photoexcitation, these values rapidly become much less significant than other terms and thus can be excluded from eqn (9.18); (ii) $[e_R]$ and $[h_R]$ represent the number of electrons and holes trapped by the recombination centers, R – in the case of fast recombination these quantities can be assumed to be equal to each other and thus can be subtracted from eqn (9.18); (iii) $[e_{v_a}]$ and $[h_{v_c}]$ denote the number of electrons and holes trapped by the corresponding defect centers (for instance, anion and cation vacancies) resulting in the formation of **F**- and **V**-type color centers; (iv) $[e_v]$ and $[h_F]$ refer to the number of electrons and holes trapped by the corresponding color centers through which complete recombination can occur; and (v) $[e_A]$ and $[h_D]$ are the number of electrons and holes involved in the surface chemical reactions with acceptor and donor reagent molecules, respectively.

Accordingly, regrouping the terms in eqn (9.18) yields:

$$([e_{v_a}] - [h_F]) + [e_A] = ([h_{v_c}] - [e_v]) + [h_D] \quad (9.19)$$

that is:

$$[\mathbf{F}] + [e_A] = [\mathbf{V}] + [h_D] \quad (9.20)$$

since $[e_{v_a}] - [h_F] = [\mathbf{F}]$ is the amount of photogenerated electron color centers, and $[h_{v_c}] - [e_v] = [\mathbf{V}]$ is the amount of photogenerated hole color centers. Eqn (9.20) thus establishes the correlation between the number of photoinduced color centers and the number of reagent molecules involved in the surface chemical reaction. Clearly, in the case of true photocatalysis

(see Scheme 9.3a), for which $[e_A] = [h_D]$, the condition for the photocoloration of the metal–oxide sample is the same with or without any surface reaction; that is, $[F] = [V]$. This correlation was clearly demonstrated by Emeline and coworkers¹⁰ as shown in Figure 9.2.

As evident in Figure 9.2, the level of photoinduced coloration is approaching that observed during irradiation *in vacuo* ($\Delta R \rightarrow 0$) when the rate of photoreaction is reaching the stationary state ($dP/dt \rightarrow \text{const}$), as is typical for catalytic process, and means that $[e_A] = [h_D]$. Otherwise, if the surface photoreaction is not a catalytic process, that is if $[e_A] \neq [h_D]$, then the number of electron color centers would also not equal the number of hole color centers in the solid, that is $[F] \neq [V]$.^{10,16,17}

Indeed, as shown in Figure 9.3 for such a typical non-catalytic processes as the photostimulated adsorption of hydrogen or oxygen, the level of photocoloration (photoinduced defect formation) and the absorption spectra of photoinduced defects are significantly different compared to those observed under irradiation *in vacuo*.

In accordance with the charge balance eqn (9.20), the photostimulated adsorption of electron-donor hydrogen molecules results in the enhancement of the absorption by electron defects whereas photostimulated adsorption of electron-acceptor oxygen molecules leads to a decrease of the F-type center absorption. Thus, a non-photocatalytic surface reaction affects the process of formation of photo-induced color centers by changing the relationship between electron and hole color centers. The more pronounced the non-photocatalytic character of the surface reaction is, the stronger is the deviation of the relation $[F] \neq [V]$ from equality. Accordingly, monitoring the photocoloration of the solid during the surface photochemical reaction provides a possible evaluation as to whether the photochemical process

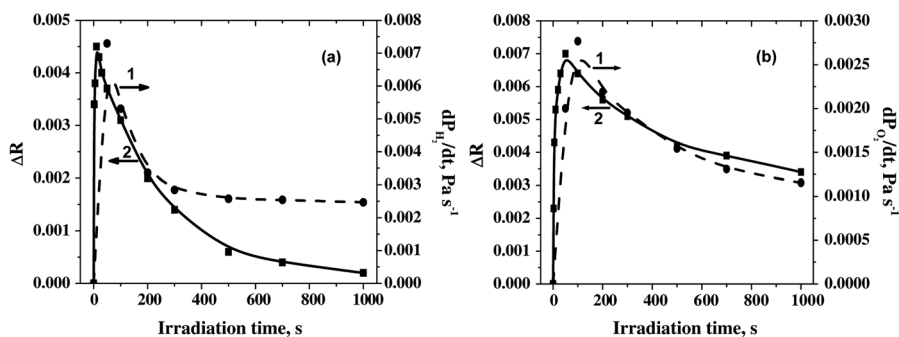


Figure 9.2 (a) Time evolutions of the hydrogen consumption rate (1) during photocatalytic hydrogen oxidation over ZrO_2 and alteration of the amount of the hole (V-type) color centers (2) compared with to irradiation *in vacuo*; (b) time evolutions of the oxygen consumption rate (1) during photocatalytic hydrogen oxidation over ZrO_2 and alteration of the amount of the electron (F-type) color centers (2) compared with irradiation *in vacuo*. (Reproduced from ref. 10. Copyright 2005 American Chemical Society.)

is photocatalytic and to what the extent of photocatalysis might be. As an example one may consider the study of photoprocesses of ammonia photolysis and its effect on photoinduced defect formation in a spinel reported elsewhere.¹⁷ Photolysis of pre-adsorbed ammonia results in the formation of hydrazine (Figure 9.4) as an intermediate product followed by the evolution of gaseous nitrogen. Monitoring of the photoinduced V-type defect formation (Figure 9.5) indicates that the kinetics of defect accumulation during the photolysis of ammonia are very similar to the those during the

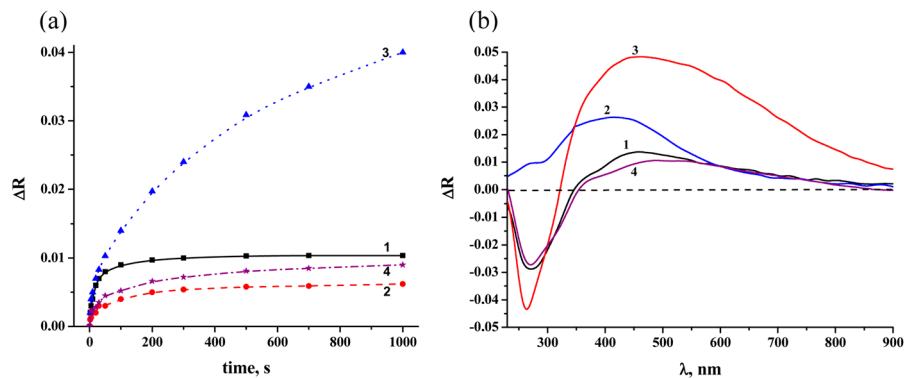


Figure 9.3 (a) Kinetics of accumulation of the electron F-type color centers during photo-irradiation of ZrO_2 in vacuo (1), in the presence of oxygen (2), hydrogen (3), and a mixture of oxygen and hydrogen (4). (b) Difference diffuse reflectance spectra (corresponding to absorption spectra) of photoinduced color centers after photo-irradiation of ZrO_2 in vacuo (1), in the presence of oxygen (2), hydrogen (3), and a mixture of oxygen and hydrogen (4). (Reproduced from ref. 10. Copyright 2005 American Chemical Society.)

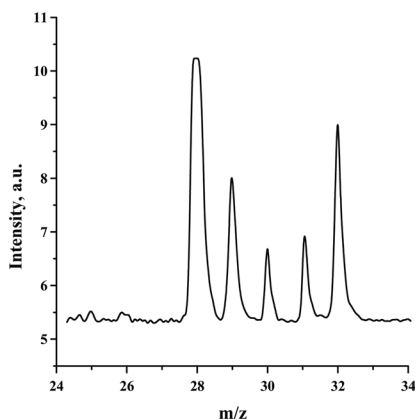


Figure 9.4 Mass-spectrum of hydrazine formed at the surface of a spinel during photolysis of ammonia. (Reproduced from ref. 17. Copyright 2012 American Chemical Society.)

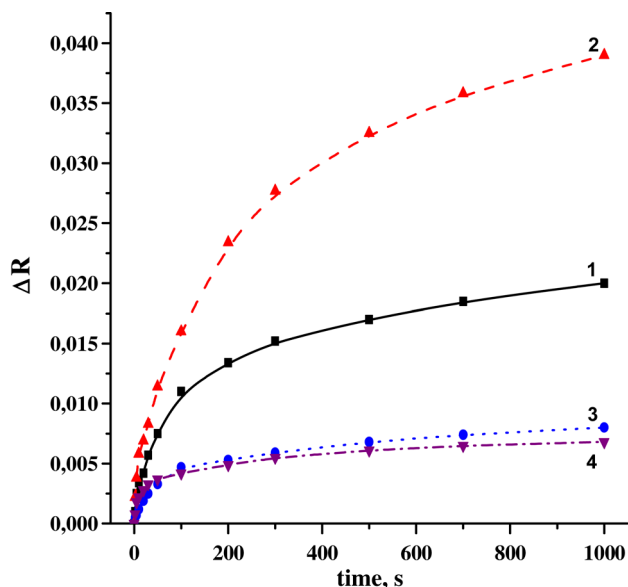


Figure 9.5 Kinetics of photoinduced formation of hole V-type color centers after irradiation *in vacuo* (1), in the presence of oxygen (2), hydrogen (3), and pre-adsorbed ammonia (4). (Reproduced from ref. 17. Copyright 2012 American Chemical Society.)

photostimulated adsorption of hydrogen and differs from the kinetics of defect formation during the irradiation of spinel *in vacuo* or in the presence of oxygen. Thus, on the basis of the charge balance one may conclude that the photolysis of ammonia is a non-catalytic process and involves the interaction with surface hole states only (similar to the photostimulated adsorption of hydrogen).

Therefore, the interconnection between physical photoprocesses of defect formation and surface photochemical reactions based on the total charge balance provides information about whether the surface reaction is catalytic or not, and if it is not then which reaction pathway (either reductive or oxidative) is the dominant one.

9.4 Interconnection Between the Activity and Selectivity of Photocatalysts

9.4.1 Activity of Photocatalysts

To gain further insight into the interplay between the physical and chemical photostimulated events in heterogeneous systems we now consider the factors that may govern the activity and selectivity of the photocatalyst; we also consider the interconnection between photoexcitation and charge transport in solids and variation of the chemical behavior of the surface.

As mentioned in the previous section, at a high concentrations of reagent (which means that the high concentrations provide the conditions under which decay of the active centers through recombination is suppressed by the chemical step) the rate of the process becomes:

$$\text{Rate} = k_{tr}[S]n_s \quad (9.21)$$

Then, the quantum yield represents basically the efficiency of photogeneration of surface-active centers as suggested by eqn (9.22), which indicates that under the applied conditions the quantum yield depends on k_{tr} , the concentration of surface-active centers, S , and the surface concentration of charge carriers, n_s :

$$\Phi = \frac{k_{tr}[S]n_s}{A\rho} \quad (9.22)$$

Therefore, the activity of photocatalysts characterized by the quantum yield, which represents the ability of photoactive materials to transform the physical event of light absorption into a surface chemical reaction, depends on physical characteristics such as surface concentration of photogenerated charge carriers, physical-chemical characteristics of the surface structure represented by the surface concentration of surface-active centers and on a chemical parameter – the reaction rate constant.

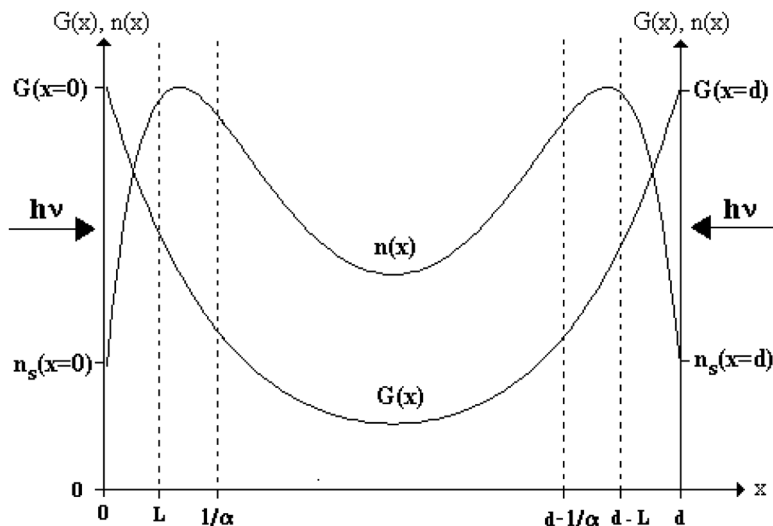
The surface concentration of free charge carriers can be found from the solution to the continuity equation under the steady-state approximation:

$$\frac{\partial n(x,t)}{\partial t} = -\frac{\partial J_n(x,t)}{\partial x} - \frac{n(x,t)}{\tau} + G(x,t) = 0 \quad (9.23)$$

The solution to the continuity eqn (9.23) for a one-dimensional infinite plate model (Scheme 9.5) taking into consideration a non-uniform function of carrier generation that obeys the Lambert-Beer law and with diffusion as the major path of carrier flow gives the spatial distribution of carriers in the bulk of the solid (Scheme 9.4). The expression for the surface concentration of carriers is:¹⁸

$$n_s = \frac{2(1 - e^{-\alpha d})\chi\rho\alpha L^2}{D \left[\tanh\left(\frac{d}{2L}\right) + \zeta \right] (1 - \alpha^2 L^2)} \left[\tanh\left(\frac{d}{2L}\right) \coth\left(\frac{\alpha d}{2}\right) - \alpha L \right] \quad (9.24)$$

where α is the absorption coefficient of the solid, d is the thickness of the plate, $L = (D\tau)^{1/2}$ is the diffusion length of carriers, and ζ is a ratio of rates of surface to bulk recombinations. Substitution of the surface concentration of carriers (eqn (9.24)) into eqn (9.21) for the reaction rate, followed by substitution of the resulting expression into eqn (9.22) for the quantum yield [where $A = 2(1 - e^{-\alpha d})$ for the infinite plate irradiated from both sides] results in the expression for the quantum yield (Φ) of the primary surface chemical process:



Scheme 9.5 Scheme of an infinite solid plate with thickness (d) irradiated uniformly from both sides. The curve $G(x)$ describes a non-uniform spatial distribution of carrier photogeneration. The straight vertical lines between the surface and the bulk define a depth equal to the average diffusion length of the carriers L and average length $1/\alpha$ of light penetration into the bulk. The carriers generated within the diffusion length can reach the plate surfaces by diffusion migration. Those generated in the remaining part of the lattice bulk cannot take part in surface chemical processes. The curve $n(x)$ represents the spatial distribution of the concentration of free charge carriers. (Reproduced from ref. 18. Copyright 1999 American Chemical Society.)

$$\Phi = \frac{k_{tr} S \chi \rho \alpha L^2}{D \left[\tanh\left(\frac{d}{2L}\right) + \zeta \right] (1 - \alpha^2 L^2)} \left[\tanh\left(\frac{d}{2L}\right) \coth\left(\frac{\alpha d}{2}\right) - \alpha L \right] \quad (9.25)$$

where S is the concentration of surface-active sites (e.g. surface OH^- groups or surface electron traps, Ti^{4+}) and k_{tr} corresponds to either k_{11} or to k_{15} , respectively.

Eqn (9.25) suggests that a spectral variation of the absorption coefficient (α) leads to a spectral variation of the quantum yield of a chemical process, and therefore the variation of the physical behavior of the photoactive materials results in the alteration of photocatalyst activity. A detailed analysis of the general expression (9.25) and the most important specific scenarios of the strong fundamental absorption and weak extrinsic absorption for the variation of photocatalyst activity is given elsewhere.¹⁸⁻²⁰ Some significant inferences can be made, however, as summarized below:

- The quantum yield (Φ) of the surface reaction depends on the ratio d/L , that is the bulk fraction from where the photogenerated charge carriers are able to reach the surface and participate in the interfacial chemical events. The smaller d/L is, the smaller is the fraction of carriers in the bulk that diffuse to the surface, and hence the greater is the fraction of absorbed photons that are inactive.
- The greater the mobility of carriers is (thus the longer the diffusion length L), the greater is Φ for a given crystal size d and absorption coefficient α . The smaller the size of particles' d is, the smaller is the ratio d/L , and the greater Φ will be.
- The quantum yield scales sub-linearly with αL , expressing the ratio between that part of the solid bulk where the photogeneration of charge carriers occurs and that part of the bulk from which the carriers can reach the surface as a result of diffusion. Note, that αL and αd reflect the spatial non-uniformity of the light distribution and therefore the charge carrier photogeneration in the bulk of the photocatalyst particles.

Complex events take place when the absorption spectra of solids consist of the overlap of several single absorption bands belonging to different types of light absorption, and that differ either (a) by their abilities to form free carriers (internal quantum yield of photo-effect) or/and (b) by the properties (mobility, lifetime) of newly generated carriers. We have demonstrated experimentally²⁰ that the former cause (a) is essential for weak *extrinsic* light absorption by defects, which leads to band-like or step-like spectral dependencies of the quantum yields whose shape is dictated by the degree of overlap of single absorption bands of different types, whereas the latter reason (b) becomes important in the spectral range of *intrinsic* (fundamental) light absorption by the solid when the hot carriers generated at a photon energy greater than the bandgap energy are involved in surface processes. In such a case, in addition to the spectral variations of Φ caused by the spectral variation of the absorption coefficient α , especially at the fundamental absorption edge, the spectral dependence of Φ may also be attributed to the spectral variation of the mobilities and lifetimes of carriers generated at different wavelengths (see eqn (9.25)) owing to different direct and indirect band-to-band transitions that result in different initial population of the electronic states in bands. A particular example of the spectral variation of the photocatalyst activity is shown in Figure 9.6.

In the spectral region of the weak extrinsic absorption when $\alpha L \rightarrow 0$, eqn (9.25) transforms into eqn (9.26):

$$\Phi = \frac{2k_{tr}S_0\chi L^2}{Dd} \left[\frac{\tanh\left(\frac{d}{2L}\right)}{\tanh\left(\frac{d}{2L}\right) + \zeta} \right] \quad (9.26)$$

indicating that the quantum yield becomes independent of the absorption coefficient and therefore on its spectral variation. In other words, within the single absorption band when the mechanism of photoexcitation remains the same, the quantum yield is a constant.^{18–20} Accordingly, any experimentally observed spectral dependence of the quantum yield of surface photoreactions (see, for example, Figure 9.7) infers that the light absorption in the extrinsic spectral region is rather complex and is formed by the overlap of

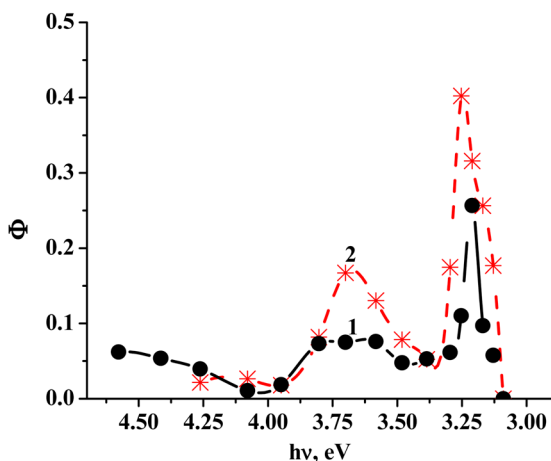


Figure 9.6 Spectral dependencies of the quantum yield of the photodegradation of phenol (1) and 4-chlorophenol (2) over TiO_2 (P-25). (Reproduced from ref. 21. Copyright 2000 American Chemical Society.)

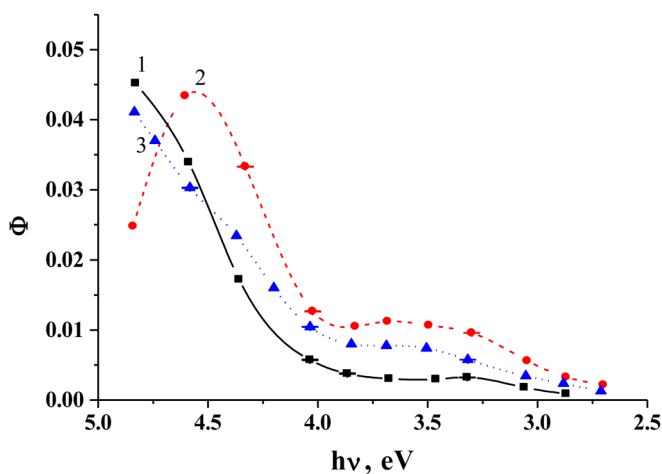


Figure 9.7 Spectral dependencies of the quantum yields of oxygen reduction (1), and hydrogen (2) and methane (3) photo-oxidation on powdered ZrO_2 . (Reproduced from ref. 20. Copyright 2000 American Chemical Society.)

several single absorption bands corresponding to different photoexcitation mechanisms (photoexcitation of different electronic states).

Formally, it can be presented by eqn (9.27):

$$\Phi = \frac{\sum_i R_i}{\rho \sum_i A(\lambda)_i} = \frac{\sum_i \Phi_i A(\lambda)_i}{\sum_i A(\lambda)_i} \quad (9.27)$$

where Φ_i = constant corresponds to the quantum yield within a given i -single absorption band $A(\lambda)_i$. Therefore, the shape of the spectral dependence of the quantum yield is dictated by the degree of the overlap of the single absorption bands forming the spectrum of extrinsic absorption of the photocatalyst.

Thus, the chemical activity of the photocatalyst surface is strongly affected by the physical (optical and electronic) characteristics of the bulk and the surface of solids in accordance with Scheme 9.1.

9.4.2 Selectivity of Photocatalysts

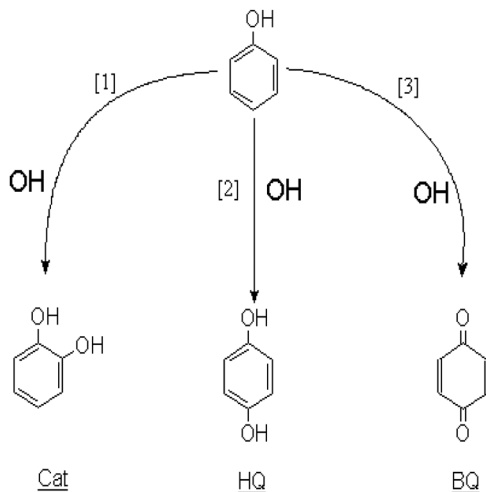
One of the important characteristics of photocatalysts is the surface selectivity, which can be described briefly as the ability of photocatalysts to turn the reaction pathway toward certain reaction products. It can be defined as the ratio between the number of molecules of reactions products formed during the reaction and the number of reagent molecules that have been involved in the reaction. However, since the reaction rates of the degradation of the reacting substrate(s) and of the formation of products can vary during the time course of the reaction, it is wise to use the ratio between the rates of formation of products, dN_i/dt , and the rate of the disappearance of reagent(s), dN_r/dt , at a given time period. Clearly, the ratio of the rates is equivalent to the ratio between the quantum yields of product formation (Φ_i) and reagent degradation (Φ_r) as noted in eqn (9.28):

$$S_i = \frac{dN_i/dt}{dN_r/dt} = \frac{\Phi_i}{\Phi_r} \quad (9.28)$$

Two different factors affecting the surface selectivity of photocatalysts have been demonstrated earlier.^{22,23} The first factor can be illustrated well by the formation of major primary intermediates (catechol (1 – Cat), hydroquinone (2 – HQ), and benzoquinone (3 – BQ)) during phenol photodegradation (Scheme 9.6).

All the primary intermediates are formed through the oxidation pathway of phenol degradation only occurring through the interaction with photo-generated OH radicals.^{22,24} Accordingly, the selectivity toward formation of the intermediates can be represented as:

$$S_{\text{HQ}} = \frac{d[\text{HQ}]/dt}{d[\text{PhOH}]/dt} = \frac{k_{\text{HQ}} [\text{OH}][\text{PhOH}]}{\sum_i k_i [\text{OH}][\text{PhOH}]} = \frac{k_{\text{HQ}}}{\sum_i k_i} \quad (9.29a)$$



Scheme 9.6 Formation of the major primary intermediates (catechol (1 - Cat), hydroquinone (2 - HQ), and benzoquinone (3 - BQ)) during the phenol photo-oxidation. (Reproduced from ref. 22. Copyright 2002 American Chemical Society.)

$$S_{\text{Cat}} = \frac{d[\text{Cat}]/dt}{d[\text{PhOH}]/dt} = \frac{k_{\text{Cat}}}{\sum_i k_i} \quad (9.29b)$$

$$S_{\text{BQ}} = \frac{d[\text{BQ}]/dt}{d[\text{PhOH}]/dt} = \frac{k_{\text{BQ}}}{\sum_i k_i} \quad (9.29c)$$

Thus, the selectivity is dictated only by chemical factors that are ratios between corresponding rate constants, and its alteration does not depend on the physical parameters. Indeed, such independence can be illustrated (Figure 9.8) by experimental results that show that the selectivity remains constant within a wide spectral range of the fundamental absorption of TiO_2 .

This behavior can be explained in terms of the reactive oxidative species ($\cdot\text{OH}$ radicals) formed due to trapping of free holes generated by band-to-band transitions by surface hydroxyl groups, and therefore their nature remains independent of the physical characteristics of solids and depends on the surface chemistry only (Scheme 9.6). However, phenol degradation becomes more complex in the case of extrinsic light absorption when different mechanisms of photoexcitation result in the formation of different hole states at the surface possessing different reactivity that is characterized by different reaction rate constants (k_i) (Scheme 9.7).

Then, the alteration of the reaction rate constants with variation of the wavelength of photoexcitation leads to the spectral variation of the photocatalyst selectivity as shown in the Figure 9.9.

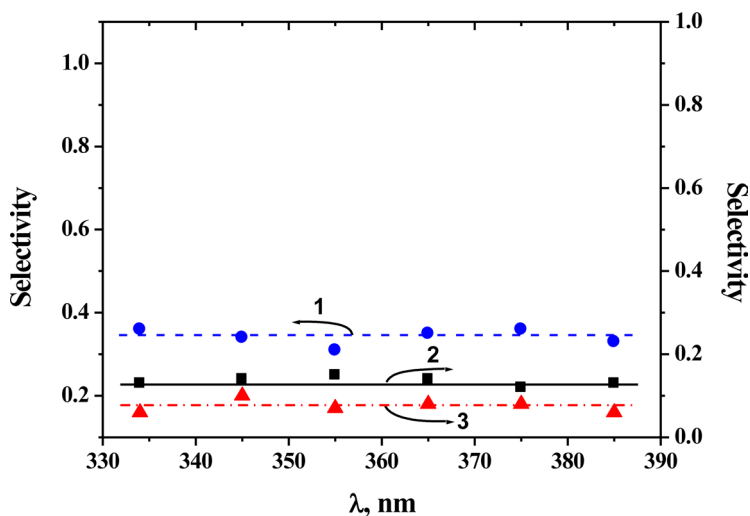
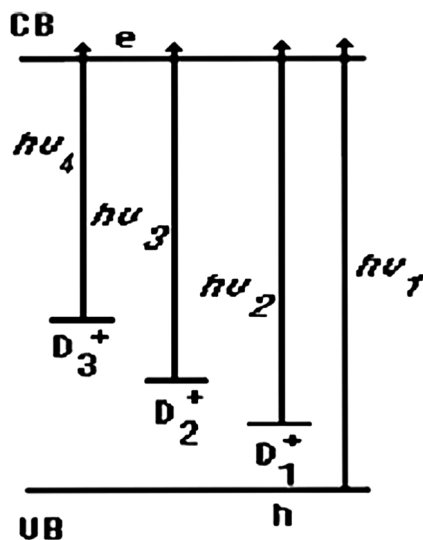


Figure 9.8 Spectral dependencies of the initial selectivity toward the formation of hydroquinone (1), catechol (2), and benzoquinone (3) during the photocatalytic degradation of phenol over TiO_2 (Degussa P25). (Reproduced from ref. 22. Copyright 2002 American Chemical Society.)



Scheme 9.7 Mechanism of photoexcitation in intrinsic and extrinsic absorption spectral regions resulting in the formation of different surface hole states (surface-active centers).

Note that this observation is in agreement with eqn (9.28), indicating that the spectral variation of the selectivity should scale with alteration of the ratio of the quantum yields of product formation and reagent consumption, which in turn depends on the alteration of the excitation mechanism.

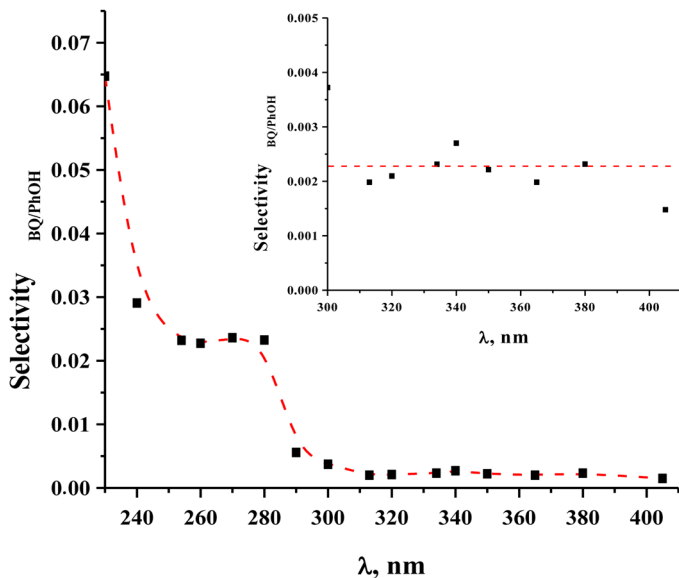
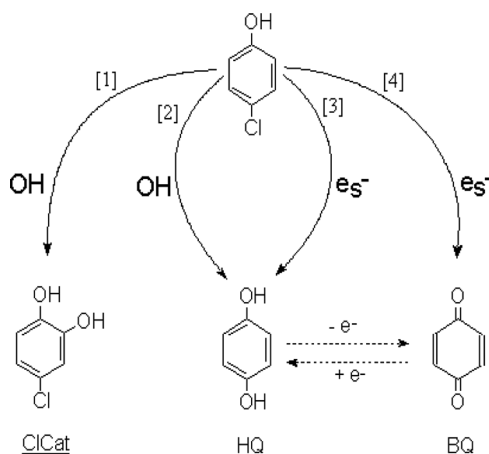


Figure 9.9 Spectral variation of the selectivity towards formation of hydroquinone during phenol photodegradation over ZrO_2 .



Scheme 9.8 Formation of the primary major intermediates (4-chlorocatechol, hydroquinone, and benzoquinone) during 4-chlorophenol photodegradation. (Reproduced from ref. 22. Copyright 2002 American Chemical Society.)

Another factor affecting the selectivity of photocatalyst surface²² can be demonstrated with the example of 4-chlorophenol photodegradation and formation of the primary major intermediates: 4-chlorocatechol, hydroquinone, and benzoquinone (Scheme 9.8).

The photodegradation of 4-chlorophenol goes through both oxidation and reduction pathways.^{25,26} Therefore, the ability of photocatalysts to promote

either reductive or oxidative surface reactions depends on the ratio between the surface concentrations of electrons and holes. Since surface concentrations of both types of carriers are spectrally dependent (eqn (9.24)), their ratio is generally also spectrally dependent. This may cause a spectral variation in photocatalyst selectivity.

According to the simple model of surface photochemical reactions illustrated by Scheme 9.8, if reductive and oxidative processes (*i.e.* interaction of reagent molecules with electrons and holes, respectively) take place only on the photocatalyst surface, then the selectivity toward product formation by the reductive pathway can be expressed by eqn (9.30) and for product formation through the oxidative pathway by expression (9.31):

$$S_{\text{red}} = \frac{k_{\text{red}} [e][M]}{(k_{\text{red}} [e] + k_{\text{ox}} [h])[M]} = \frac{\gamma}{\gamma + \frac{k_{\text{ox}}}{k_{\text{red}}}} \quad (9.30)$$

$$S_{\text{ox}} = \frac{k_{\text{ox}} [e][M]}{(k_{\text{red}} [e] + k_{\text{ox}} [h])[M]} = \frac{\frac{k_{\text{ox}}}{k_{\text{red}}}}{\gamma + \frac{k_{\text{ox}}}{k_{\text{red}}}} \quad (9.31)$$

Two parameters stand out that affect the selectivity S_i : (a) the ratio of the rate constants for oxidation and reduction and (b) the parameter γ , which expresses the ratio between the surface concentrations of electrons and holes, *i.e.* $\gamma = [e_s]/[h_s]$. An analysis of expressions (9.30) and (9.31) leads to some important inferences:

- The selectivity for reduction (S_{red}) increases with an increase in γ (increase in the number of surface electrons).
- The selectivity for oxidation (S_{ox}) scales with $1/\gamma$.
- The degree of variation in selectivities depends on the ratio $k_{\text{ox}}/k_{\text{red}}$.
- When $\gamma \ll k_{\text{ox}}/k_{\text{red}}$ the selectivity is shifted toward the oxidative path.
- When $\gamma \gg k_{\text{ox}}/k_{\text{red}}$ the reductive pathway is the favored path.

Clearly, the ratio between the surface concentrations of electrons and holes, $[e_s]/[h_s]$, is the important factor that determines the selectivity of photocatalysts. On application of the models of the infinite plate (Scheme 9.5) and the results obtained for the surface concentration of charge carriers, an analysis can be made of the behavior of photocatalysts during photochemical reactions. Thus, the model(s) indicates that the ratio $\gamma = [e_s]/[h_s]$ is governed by various factors, among which are the:

- mobilities of the charge carriers (μ),
- lifetimes of the charge carriers (τ),
- rates of surface recombination of the charge carriers (s),

- αL expressing the ratio between that part of the solid bulk where the photogeneration of charge carriers occurs and that part of the bulk from which the carriers can reach the surface as a result of diffusion.

The latter factor can play a crucial role in the spectral variation of the selectivity since in general the diffusion lengths of electrons and holes are different. Then, the spectral variation of the absorption coefficient must result in the spectral dependence of the ratio between surface concentrations of electrons and holes, γ (see eqn (9.32)), and therefore in the alteration of the surface selectivity:

$$\gamma = \frac{[e_s]}{[·OH]} = B \frac{\alpha L_e + \beta}{\alpha L_h + 1} \quad (9.32)$$

where β is the ratio of the diffusion lengths of electrons and holes ($= L_e/L_h$).

Figure 9.10 demonstrates the experimental spectral dependence of the initial selectivity toward formation of hydroquinone, benzoquinone, and 4-chlorocatechol during 4-chlorophenol photocatalytic degradation over TiO_2 (Degussa P25).

Interestingly, benzoquinone (BQ) is formed from the interaction of 4-chlorophenol with electrons localized on the surface, whereas the ClCat (chlorocatechol) is formed by interaction of the initial substrate 4-ClPhOH with the $\cdot OH$ radicals formed by hole trapping by surface OH^- groups; hydroquinone (HQ) is formed both reductively and oxidatively. Accordingly, the selectivity

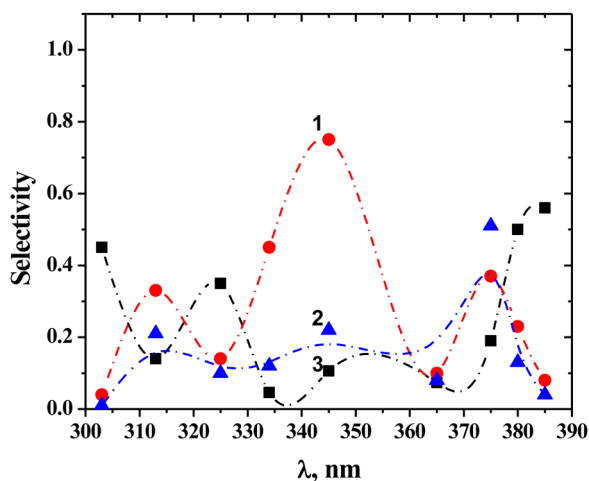


Figure 9.10 Spectral dependencies of the initial selectivity toward formation of hydroquinone (1), benzoquinone (2), and chlorocatechol (3) during 4-chlorophenol photocatalytic degradation over TiO_2 (Degussa P25). (Reproduced from ref. 22. Copyright 2002 American Chemical Society.)

of the photocatalyst can be expressed for ClCat by eqn (9.33) and for BQ by eqn (9.34):

$$S_{(\text{ClCat})} = \frac{k_1[\cdot\text{OH}]}{k'[\cdot\text{OH}] + k''[e_s]} = \frac{k_1}{k' + k''\gamma} \quad (9.33)$$

$$S_{(\text{BQ})} = \frac{k_4[e_s]}{k'[\cdot\text{OH}] + k''[e_s]} = \frac{k_4\gamma}{k' + k''\gamma} \quad (9.34)$$

Clearly, both selectivities depend on the ratio γ , and consequently on the spectral variation of γ , which causes the spectral variation of the selectivity in contrast with the degradation of phenol when all the reaction intermediates are formed through the oxidative pathway only. Interestingly, also, the ratio of the two selectivities above for the formation of BQ and ClCat, $S_{\text{BQ}}/S_{\text{ClCat}}$, scales with γ (eqn (9.35)):

$$\frac{S_{(\text{BQ})}}{S_{(\text{ClCat})}} = \frac{k_4[e_s]}{k_1[\cdot\text{OH}]} = (\text{const})\gamma \quad (9.35)$$

meaning that the spectral variation of this ratio reflects the spectral variation of the ratio between the electron and hole concentrations on the photocatalyst surface.

We showed earlier^{21,22} that the relative photonic efficiency, ζ_{rel} , for 4-chlorophenol degradation over titania with respect to the degradation of phenol also scales with γ . The spectral dependencies of ζ_{rel} and of the ratio $S_{\text{BQ}}/S_{\text{ClCat}}$ are illustrated in Figure 9.11. Clearly, the two dependencies correlate with each other, as expected theoretically.

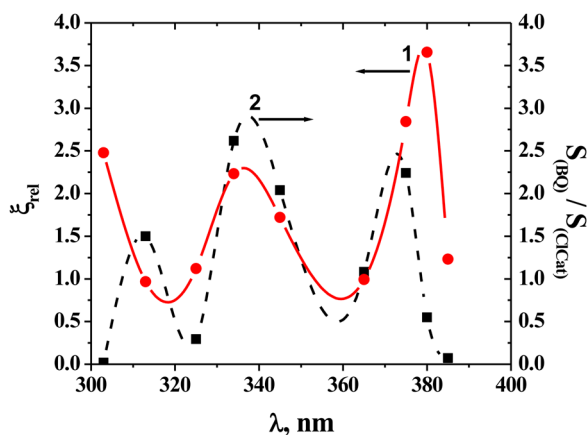


Figure 9.11 Spectral dependencies of the relative photonic efficiency of the photodegradation of 4-chlorophenol (1) and of the ratio between the initial selectivity of the formation of benzoquinone and chlorocatechol, $S_{(\text{BQ})}/S_{(\text{ClCat})}$, (2) which scales with γ .

Therefore, when the surface photoreaction is taking place through both oxidation and reduction pathways, alteration of the efficiency of photophysical processes will strongly affect the surface chemistry, particularly the selectivity of photocatalyst surface.

Recently, the correlation between activity and selectivity of a photocatalyst has been demonstrated by Emeline *et al.*²⁷ in the photodegradation of 4-chlorophenol taking place over irradiated TiO_2 . A strong positive correlation ($r = 0.984$; $p = 0.0004$) was observed (Figure 9.12) between selectivity toward formation of hydroquinone and the activities of the photocatalyst.

According to the charge balance, as expressed by Gerisher and Heller,²⁸ the true (photo)catalytic process is characterized by the equality of the rates of consumption of electrons and consumption of holes in the overall reaction (eqn (9.5a)). This charge balance represents the required condition for the effective photocatalytic process. Otherwise, deviation from the catalytic equilibrium (eqn (9.5a)) would result in the transformation of the charge balance according to eqn (9.20), where F and V denote the electrons and holes, respectively, trapped by bulk defects (color centers), which lead to acceleration of the bulk charge recombination and to the decrease of the activity of the photocatalyst. Since formation of hydroquinone effectively consumes both electrons and holes, these reaction pathways create a favorable condition for the photodegradation of 4-chlorophenol that is truly photocatalytic and suppressing bulk recombination. Therefore, the higher the selectivity of the photocatalyst surface toward formation of hydroquinone, the higher is the activity of the photocatalyst during the 4-chlorophenol

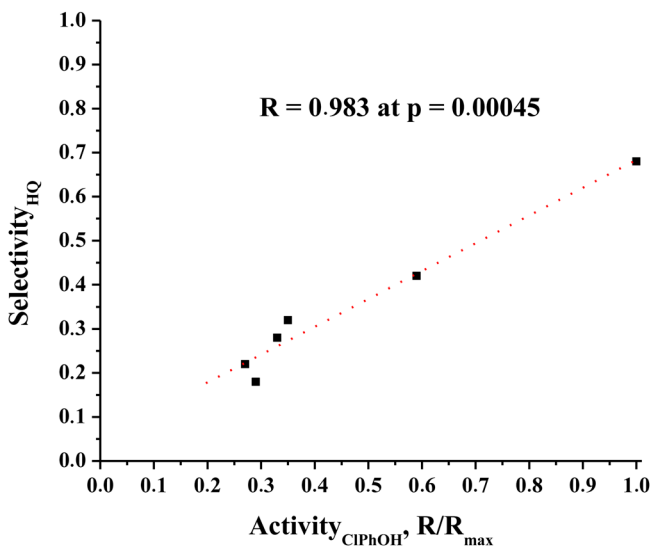


Figure 9.12 Correlation between selectivity toward formation of hydroquinone and the activities of the different TiO_2 photocatalysts. (Reproduced from ref. 27. Copyright 2012 Elsevier.)

photodegradation. In general, this rule can be formulated as a higher activity of photocatalysts can be expected provided that both reduction and oxidation reaction pathways occur with equally high efficiency. In turn, this requires a good agreement in the interplay between physical and chemical photoprocesses.

9.5 Concluding Remarks

In this chapter we have briefly examined theoretical considerations and experimental evidences for correlations between physical and chemical characteristics of photostimulated processes in heterogeneous systems indicating a strong interplay between them. The creation of new generations of photoactive materials will lead to successful applications only if such interplay between physical and chemical processes is taken into account fully.

Acknowledgements

The writing of the present chapter was undertaken within the Project “Establishment of the Laboratory ‘Photoactive Nanocomposite Materials’” (No. 14.Z50.31.0016, Mega-grant from the Government of the Russian Federation) and supported by Research Program of Saint-Petersburg State University (No. 11.38.207.2014).

References

1. A. N. Terenin, *Acta Physicochem. URSS*, 1936, **1**, 407.
2. D. DeBeur, *Electron Emission and Adsorption Phenomena*, 1936, p. 315.
3. X. Chen and S. S. Mao, *Chem. Rev.*, 2007, **7**, 2891.
4. J. Schneider, M. Matsuoka, M. Takeuchi, J. Zhang, Y. Horiuchi, M. Anpo and D. W. Bahnemann, *Chem. Rev.*, 2014, **114**, 9919.
5. A. Fujishima, K. Hashimoto and T. Watanabe, *TiO₂ Photocatalysis: Fundamentals and Applications*, BKC Publishing, Tokyo, 1999.
6. M. Gratzel, *J. Photochem. Photobiol., C*, 2003, **4**, 145.
7. *Solar Photon Conversion in Nanostructured and Photoelectrochemical Systems*, ed. M. D. Archer and A. J. Nozik, Imperial College, 2008, p. 592.
8. K. Nakata, T. Ochiai, T. Murakami and A. Fujishima, *Electrochem. Acta*, 2012, **84**, 103.
9. A. V. Emeline, A. V. Panasuk, N. Sheremetyeva and N. Serpone, *J. Phys. Chem. B*, 2005, **109**, 2785.
10. A. V. Emeline, G. V. Kataeva, A. V. Panasuk, V. K. Ryabchuk, N. Sheremetyeva and N. Serpone, *J. Phys. Chem. B*, 2005, **109**, 5175.
11. A. V. Emeline, V. K. Ryabchuk and N. Serpone, *J. Photochem. Photobiol., A*, 2000, **133**, 89.
12. J. I. Pankove, *Optical Processes in Semiconductors*, Dover Publications, Inc., New York, 1971.

13. Ch. B. Luschnik and A. Ch. Luschnik, *Decay of Electronic Excitation with Formation of Defects in Solids*, Nauka, Novosibirsk, Soviet Union, 1989.
14. P. W. M. Jacobs and G. J. Dienes, *J. Phys. Chem. Solids*, 1990, **51**(7), v.
15. N. Serpone and R. F. Khairutdinov, Semiconductor nanoclusters – physical, chemical, and catalytic aspects, in *Studies in Surface Science and Catalysis*, ed. P. V. Kamat and D. Meisel, 1997, vol. 103, p. 417.
16. A. V. Emeline, G. V. Kataeva, A. S. Litke, A. V. Rudakova, V. K. Ryabchuk and N. Serpone, *Langmuir*, 1998, **14**, 5011.
17. A. V. Emeline, D. A. Abramkin, I. S. Zonov, N. V. Sheremetyeva, A. V. Rudakova, V. K. Ryabchuk and N. Serpone, *Langmuir*, 2012, **28**, 7368.
18. A. V. Emeline, V. K. Ryabchuk and N. Serpone, *J. Phys. Chem. B*, 1999, **103**, 1316.
19. A. V. Emeline, A. V. Frolov, V. K. Ryabchuk and N. Serpone, *J. Phys. Chem. B*, 2003, **107**, 7109.
20. A. V. Emeline, G. N. Kuzmin, D. Purevdorj, V. K. Ryabchuk and N. Serpone, *J. Phys. Chem. B*, 2000, **104**, 2989.
21. A. V. Emeline, A. Salinaro and N. Serpone, *J. Phys. Chem. B*, 2000, **104**, 11202.
22. A. V. Emeline and N. Serpone, *J. Phys. Chem. B*, 2002, **106**, 12221.
23. A. V. Emeline, X. Zhang, M. Jin, T. Murokami and A. Fujishima, *J. Photochem. Photobiol., A*, 2009, **207**, 13.
24. B. Sun, A. V. Vorontsov and P. G. Smirniotis, *Langmuir*, 2003, **19**, 3151.
25. U. Stafford, K. A. Gray and P. V. Kamat, *J. Catal.*, 1997, **167**, 25.
26. J. Theurich, M. Lindner and D. W. Bahnemann, *Langmuir*, 1996, **12**, 6368.
27. A. V. Emeline, X. Zhang, T. Murakami and A. Fujishima, *J. Hazard. Mater.*, 2012, **211–212**, 154.
28. H. Gerisher and A. Heller, *J. Phys. Chem.*, 1991, **95**, 5261.